World Academy of Science, Engineering and Technology
International Journal of Geological and Environmental Engineering
Vol:11, No:4, 2017

Ground Response Analyses in Budapest Based on Site Investigations and Laboratory Measurements

Zsolt Szilvágyi, Jakub Panuska, Orsolya Kegyes-Brassai, Ákos Wolf, Péter Tildy, Richard P. Ray

Open Science Index, Geological and Environmental Engineering Vol:11, No:4, 2017 publications.waset.org/10006887/pdf

***Abstract*—**Near-surface loose sediments and local ground conditions in general have a major influence on seismic response of structures. It is a difficult task to model ground behavior in seismic soil-structure-foundation interaction problems, fully account for them in seismic design of structures, or even properly consider them in seismic hazard assessment. In this study, we focused on applying seismic soil investigation methods, used for determining soil stiffness and damping properties, to response analysis used in seismic design. A site in Budapest, Hungary was investigated using Multichannel Analysis of Surface Waves, Seismic Cone Penetration Tests, Bender Elements, Resonant Column and Torsional Shear tests. Our aim was to compare the results of the different test methods and use the resulting soil properties for 1D ground response analysis. Often in practice, there are little-to no data available on dynamic soil properties and estimated parameters are used for design. Therefore, a comparison is made between results based on estimated parameters and those based on detailed investigations. Ground response results are also compared to Eurocode 8 design spectra.

***Keywords*—**Bender element, ground response analysis, MASW, resonant column test, SCPT, torsional shear test.

I. Introduction

LOCAL soil conditions have a great effect on earthquake motions observed at the ground surface. Eurocode 8 (EC8) and its soil classification system is used widely in Europe to obtain design spectra for modal response analysis of civil engineering structures [1]. The most important site property for classification in EC8 is the shear wave velocity of the top 30-m of soil deposit, $v_{s,30}$. Based on its value, a design spectrum is chosen which may amplify or attenuate the input seismic action. Our previous studies performed in Győr, Hungary [2] suggest that the design spectrum for soil type C given by the code may be non-conservative compared to spectra determined by 1D ground response analysis calculations from profiles obtained in field investigations.

Several studies are available in the literature concerning ground response analysis, but not many have been performed in the region of the Pannonian Basin where regional seismic risk can be considered moderate. Peak ground acceleration values between 0.08 g and 0.15 g have been determined by seismologists for the usual 10% probability of exceedance in 50 years for the seismic zones given in the Hungarian EC8 National Annex [1].

To perform ground response analysis for a site, soil profile information must first be gathered; preferably from in-situ measurements and laboratory tests. This information has a strong and direct influence on response analysis results. In this study, we used state-of-the-art soil investigation methods to obtain dynamic soil parameters: shear modulus (G), damping (D) and their variation as a function of confining stress and shearing strain level. Results from different investigation methods have been compared and their effects on ground response analysis results have been determined.

II. Study Site and Investigations Performed

The field site is located in Budapest's inner city area between a high traffic 3 by 3 lane main road and a park. It is a 300 m by 70 m area where a three-storey building will be constructed with two basement levels.

A. Site Investigation Program

The original site investigation program for the design of the building consisted of Cone Penetration Test (CPT) soundings, soil borings and laboratory tests on retrieved samples (index, oedometer, triaxial, and permeability tests).

Six CPTs were performed with depths of 18.5-22.0 m. Two of the CPTs included seismic measurements as well. Ten boreholes with similar depths were drilled as well (two 10 m, two 20 m, and six 25 m deep). The shallow boreholes and the top section of all others too were drilled dry with 180 mm spiral augers and only disturbed samples were taken. Deeper layers under the quaternary sediments were drilled with a 146-mm diameter hollow stem auger using drilling fluid with continuous sampling. These field and laboratory test results were used in the geotechnical design of the building and all data and unused samples were graciously provided by Geoplan Ltd for the scope of this study. A soil stratification model, based on the investigations and geological literature, is summarized in Table I.

No faults were found in the area; however, some variation in layer thickness appeared in the investigations, which can be considered plausible considering the relatively large site.

Geological literature revealed that the base layer of the area is a fairly inhomogeneous Miocene formation with a dominant soil type of clay – marly clay, with interbedded thinner layers of sand and silt. Above this clay, coarse-grained deposits of the Danube river can be found with varying grain size. The

Z. Szilvágyi*, O. Kegyes-Brassai, Á. Wolf, and R. P. Ray are with the Department of Structural and Geotechnical Engineering at Széchenyi István University, 9026 Győr, Hungary (corresponding author*; phone: +3630-530-4204, e-mail: szilvagyi@sze.hu).

J. Panuska is with the Department of Geotechnics at Slovak University of Technology in Bratislava, Slovakia.

P. Tildy is with the Department of Engineering Geophysics at the Geological and Geophysical Institute of Hungary.

The authors would like to acknowledge and thank the financial support of Széchenyi István University within the grant EFOP-3.6.1-16-2016-00017 for attending this conference. The authors would also like to thank Geoplan Ltd for their financial and professional support throughout this study.

Open Science Index, Geological and Environmental Engineering Vol:11, No:4, 2017 publications.waset.org/10006887/pdf

Danube channel was present in the area when tertiary layers were on the surface. Later, the channel moved westward, and the surface was a river meadow and marshland which resulted in the deposition of organic layers. Finally, the top layer is a poorly-graded fluvio-aeolic sand deposit which is covered by a thin man-made fill. The organic deposit, Layer III did not appear in all boreholes which suggests that it is not a continuous layer throughout the investigated area. The groundwater level was found at 6 m below the surface. The site was classified into Soil Class C according to EC8 and PGA in Budapest is given as 0.14 g in the National Annex.

TABLE I
STRATIFICATION MODEL OF INVESTIGATED SITE

Name	Description	Remark	Bottom lvl.
Layer I	Fill	Local, loose sandy soil	0.8-2.6 m
Layer II	Fine Sand	Poorly graded, med. dense fluvio-aeolic sand	3.6-7.8 m
Layer III	Med. plas. clay / silt	Organic deposit of marshland	6.3-7.8 m
Layer IV	Gravelly sand / sand	Danube river deposit, dense	12.1-14.6m
Layer V	Med. plas. clay / silty sand	Miocene clay with interbedded coarser grained silts, sands	at baserock ~110-150m

For this study, a more detailed investigation program was performed by the authors aimed at obtaining dynamic soil parameters as discussed in more detail in the following chapters. Our program consisted of Multichannel Analysis of Surface Waves (MASW) measurements, Bender Element (BE) tests, Resonant Column (RC), and Torsional Simple Shear (TOSS) tests. Most of these methods are capable of measuring the shear wave velocity, v_s which then can be used to obtain small strain stiffness, G_{max} as:

$$G_{max} = v_s^2 \rho \quad (1)$$

where ρ is soil mass density.

RC and TOSS tests are additionally capable of measuring the stiffness degradation and damping increase with strain, which together can be used in dynamic soil models as input parameters.

B. Multichannel Analysis of Surface Waves

In layered media, the propagation velocity of surface (Rayleigh and Love) waves depends on the frequency (or wavelength) of the wave because of geometric dispersion. This character makes it possible to derive shear wave velocity profile by inverting the phase velocity of the surface waves [3], [4]. A number of surface wave methods have been proposed for near-surface characterization by using a great variety of testing configurations, processing techniques, and inversion algorithms. One of them, the MASW method [5] is regarded as the most effective technique in urban environment, because multichannel records make it possible to separate different wave fields by applying 2D Fourier transform (in the frequency-wavenumber, *f–k* domain, see [6]) or phase shift method (in the frequency-phase velocity, *f–c* domain, see [7]) making it less sensitive to noise and coupling of receivers [8].

Although the acquisition of ground roll data seems to be an easy target, field configurations needed to be optimized for our goal; which was to image the shear wave velocity of subsurface layers down to at least 30 m. Frequency content of the records had to be low enough to obtain phase velocities at large wavelengths as well to fulfill this task. This could be reached by using low frequency geophones (with less than 10 Hz natural frequency), and high impact energy seismic sources such as weight-drop. In our case, a special source called SR-II (Kangaroo) was used for our field measurements. Pulses are generated by an 80-kg source and a blank 12-gage shotgun cartridge detonated remotely by and electric starter. In addition, a lower weight sledge hammer was also used for signal generating to complete the signal spectra towards the higher frequencies. Because of the urban environment and especially the high traffic noise, a flexible and robust shot system was developed. The acquisition layout was an array of 48 vertical geophones with 3-m spacing deployed near to the sampled boreholes and locations of CPT measurements. The shot system was similar to a diving wave tomography one, laying down source points at every third geophone supplemented by some additional offset shots. The main parameters for data acquisition are given in Table II.

TABLE II
MASW MEASUREMENT PARAMETERS

Number of channels	48
Geophone spacing	3 m
Array length	141 m
Source spacing	9 m
Source position interval	-28.5 m – 168.5 m
Sampling rate	1 ms
Receiver	4.5 Hz vertical geophones
Source	SR-II kangaroo; sledge hammer

Data processing consisted of two main steps: (i) obtaining the dispersion curves of Rayleigh wave phase velocity from the records and (ii) determining the v_s profiles. The processing was carried out by RadexPro software [9]. The records are first muted to reduce spectral leakage, the effect of random noise, and interference with other wave types, see Fig. 1.

After muting, only the surface wave component (jumping up) of the SR–II is used for *f–c* transformation by phase shift method. The dispersion curve is obtained from the (absolute and relative) maxima of the *f–c* spectrum, see Fig. 2. The *f-k* domain image gives a different viewpoint about the inherence of the linked plumes of maxima as shown in Fig. 2, which is very useful in delimiting dispersion curves.

While the shot system would have allowed carrying out a 2D processing scheme resulting in a shear wave velocity distribution section which could have followed lateral variation of layering, the low frequency contamination of high traffic noise prevented us from completing this task. Therefore, some records with low S/N ratio were selected and processed to obtain 1D v_s profiles, as shown in Fig. 3. As a general trend, the upper layers are characterized by lower shear wave velocities, and the increase of velocities is broken by a slight weakening in a depth range of 12-18 m. The increase of shear wave velocity is significant below 20 m. The

models have some scatter; two of them are illustrated in Fig. 3 representing the reliable external ones drawn together with SCPT measurements for comparison.

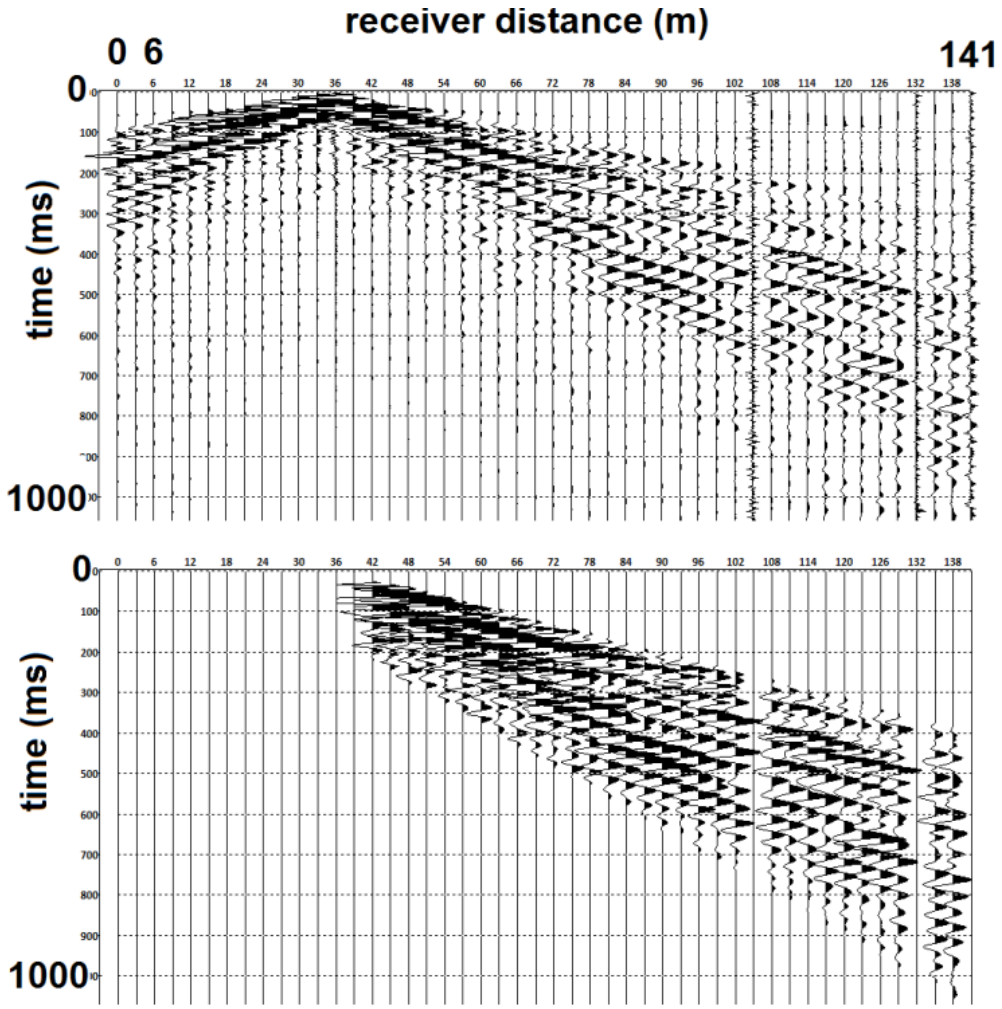


Fig. 1 Seismic record before and after tapering

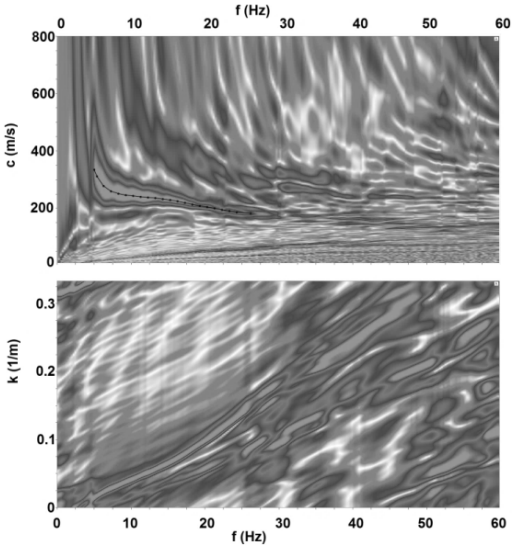


Fig. 2 Dispersion curves in f-c and f-k domain

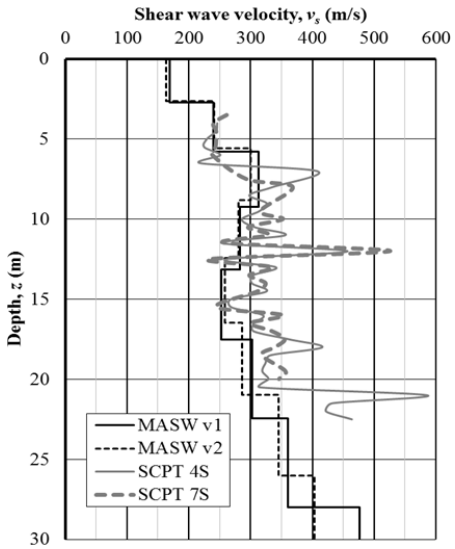


Fig. 3 Shear wave velocity profiles obtained with MASW and SCPT

Open Science Index, Geological and Environmental Engineering Vol:11, No:4, 2017 publications.waset.org/10006887/pdf

Open Science Index, Geological and Environmental Engineering Vol:11, No:4, 2017 publications.waset.org/10006887/pdf

C. Seismic Cone Penetration Testing

CPT testing is regularly used for site investigations in Hungary, because it is a quick and effective method for obtaining information about stratification, soil state and even strength and stiffness parameters. It is usually performed together with borings. By this way, correlations between in situ and lab measurements can also be made. Recently, the advantages of integrating a downhole seismic measurement into the test have also been realized by geotechnical engineers, although we cannot say that it is common practice to perform a combined test just yet.

During the SCPT test, shear wave velocity measurements were made every 0.5 m in a downhole manner. For this, a steel plate is pushed into the soil surface and a hammer is used as seismic source. Two geophones located in the cone with a separation distance of 0.5 m capture the induced waves. Wave propagation time then can be assessed based on the recorded signals; either based on the difference in first arrival of the waves or with the peak to peak method. Evaluation showed that there is marginal difference in obtained velocity values between the two methods. After obtaining the travel time, the re-phased signals can also be assessed. Shear wave velocity is finally obtained as:

$$v_s = \frac{\Delta t}{\Delta s} \tag{2}$$

where Δt is the measured travel time difference and Δs is the travel distance, i.e. the known distance between the two geophones.

In each location, at least two subsequent measurements are made in order to assure repeatability. It is beneficial to use sets of two opposite polarity shear waves, because by this way, characteristic points of the signal can be more easily identified. During the assessment, one has to take into account that the results obtained for the top 2-3 m have an inherent uncertainty because the source is usually located with an offset of a couple of meters to the cone rod. This means that travel distance close to the surface has to be assessed based on the geometry of the setup, although this is often neglected. Due to these uncertainties, we discarded the measurement results in this zone.

As outlined before, six CPTs were performed for this study with two of them having the extension of shear wave velocity measurement. During evaluation of all six CPTs it was observed, that (i) the organic deposit Layer III only appeared in one of the CPTs; (ii) there is quite a bit of scatter in the cone resistance in Layer IV while (iii) in all other layers the six measurements showed smaller variations in cone resistance. This may be due to different content of the gravel fraction in Layer IV over the investigated area. Fig. 3 shows the two shear wave velocity profiles.

In many cases in practice, especially for smaller projects, SCPT is not feasible. In such cases, it can be highly advantageous if regular CPT data can be used to estimate shear wave velocity. For this, the applicability of existing correlations in literature, such as [10], [11] should be assessed for local soils. These are generally based on statistical analyses of site investigation of a particular location. Some of them showed that, in addition to CPT measured data, the geologic age and the void ratio havr significant effect on the accuracy of estimations. On the other hand, void ratio is not available in most cases; therefore, our estimates are based only on CPT data.

There are several suggestions for different geologic age soils. Reference [12] suggests to estimate shear wave velocity correlations given in [10] for similar geological condition as the investigated site, based on a comprehensive comparison study of existing recommendations in the literature. According to [10], the shear wave velocity can be calculated as

$$v_s=(10^{0.55I_c+1.68}(q_t-\sigma_{v0})/p_a)^{0.5} \tag{3}$$

where I_c is the soil type behavior index calculated from CPT measured data [13], q_t is the cone tip resistance corrected for pore pressure, σ_{v0} is the total overburden stress, and p_a is the atmospheric pressure.

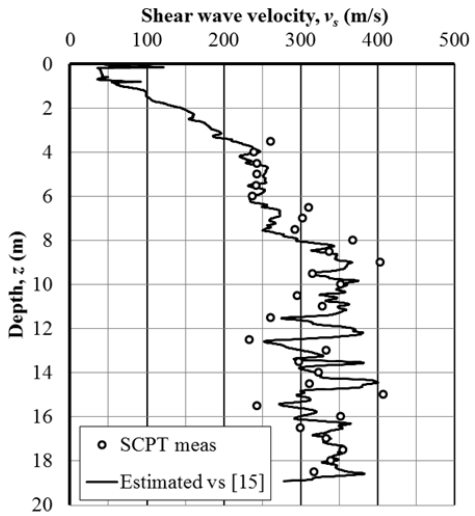


Fig. 4 Measured and estimated shear wave velocity profile

The estimated v_s profile showed good agreement with measured data for both SCPTs. One of the profiles is shown in Fig. 4.

D. Bender Element Testing

Measurements of shear wave velocity on three undisturbed samples of clay from Layer V were performed by bender elements (BE). Bender elements consist of two piezo-ceramic elements: a sender and a receiver. When voltage is applied to the sending element on one end of the sample, it bends and performs shear like movement. This movement induces shear waves in the sample propagating with shear strains in the order of 10^{-3}% [14]. The receiving element at the other end of the sample is excited by this movement, and it produces a voltage which is measured by an oscilloscope. Time difference between sent and received signal is travel time Δt. With the known tip-to-tip distance Δs between the elements shear wave

Open Science Index, Geological and Environmental Engineering Vol:11, No:4, 2017 publications.waset.org/10006887/pdf

velocity is calculated as given in (2). This technique for measuring v_s was proved by the installation of the elements in an RC device and comparing values of v_s obtained by RC and BE [15], [16].

In the present study, BE were installed in the top cap and bottom pedestal of a Bishop and Wesley triaxial cell. In the setup used, BE are able to produce both shear and compression waves [15], but for this study just shear waves were measured. Penetration of elements into the sample was 2 mm. Samples were tested under isotropic confinement with mean effective stress *p'* from 50 kPa to 600 kPa. At least four stress levels in this range were tested for one sample to find out the relation between v_s and *p'*. Effect of the stress anisotropy on v_s for clay samples is negligible according to literature [16], [17].

Three types of excitation signals were used with a peak to peak amplitude of 28 V. Signals used were: single sine wave, four sine waves, and linear sine sweep. Frequency of signals varied from 3 kHz to 20 kHz for sine waves, from 10 kHz to 17 kHz for four sine waves signal, and from 5 kHz to 50 kHz for sine sweep. All of these different signals and frequencies used were chosen to reveal the behavior of the whole system (triaxial device assembly – bender elements – soil sample) and side effects such as dispersion [18], [19], near field effect and overshooting [14]. A signal stacking procedure was used with 20 stacks per one measurement to reduce the noise in the signal.

Three evaluation methods were used to evaluate Δt and thus v_s: (i) Time domain analysis by the peak-to-peak method; (ii) cross correlation [18]-[20]; and (iii) frequency domain analysis in means of the measurement of phase shift between the two signals [14], [18] with moving frequency window algorithm [20]. These methods were incorporated in MATLAB code to automate the procedure. Measured values of v_s with the different evaluation methods usually varied in the range of max. ±10 m/s. These single measurement values were then averaged. Evaluation of the BE measurements will not be discussed further here as this topic will be elaborated in the future in a separate paper.

Physical properties of tested samples are given in Table III.

TABLE III
PHYSICAL PROPERTIES OF TESTED SAMPLES - BE TESTS

Sample ID (depth - m)	*L* - *D* (mm)	*e* (-)	S_r (%)	ρ_s (g/cm^3)
S1 (22.1 - 22.6)	101.44 - 49.60	0.88 - 0.81	84.9	2.829
S2 (23.6 - 24.1)	91.57 - 49.94	0.58 - 0.50	88.8	2.778
S3 (17.6 - 18.1)	67.49 - 49.25	0.68 - 0.63	88.2	2.819

In Table III, *L* - *D* is length and the diameter of the sample, *e* is void ratio, S_r is saturation level, and ρ_s is mass density. The void ratio range is given as value before testing and after the application of the highest confinement. Differences in sample lengths are caused by the difficulty to obtain undisturbed samples of the stiff and brittle clay material. Small holes for the elements were carved on both ends of the sample and they were filled up with silicon grease to maintain the contact and ensure the transfer of movement from the element to the soil. Side drains were used to speed the consolidation for all samples except for S1. After setting up the sample, the B-value was checked followed by a saturation procedure. During saturation, 20 kPa effective stress was maintained with a rate of pressure increase of 3 kPa/min to final cell pressure of 520 kPa and back pressure of 500 kPa. The B-value after the saturation was greater than 0.95 for all of the samples tested. After the successful saturation, at least four consolidation stages under isotropic confinement were conducted. Volume change was measured by measuring the volume of water leaving the sample; and height change was calculated according to isotropic state of strain, thus; 3 x axial strain = volumetric strain.

BE measurements were performed during the consolidation stage periodically and final values of v_s were obtained after primary consolidation. It was observed in [21], [22] that if primary consolidation is followed by secondary compression, the latter affects the value of v_s. Usually the increase in v_s and thus in G_{max} seems to be linear during the secondary compression (with time plotted logarithmically) and is evaluated as ratio $\Delta G/G_{1000}$ [22], [23], where ΔG is the change in the small strain shear modulus per log cycle of time, and G_{1000} is the small strain shear modulus at the end of the primary consolidation (in referenced literature taken as 1000 minutes). This effect was observed under constant effective stress and changing void ratio, but it seems not only the changing void ratio causes the increasing value of v_s and G_{max}, [22]. Unfortunately, these effects were only studied over a short period of time and not in detail. The next consolidation step was applied immediately after primary consolidation. Thus, no observations for the next log cycle of time were made. According to [17] for soils with medium grain size D_{50} > 0.04 mm, the increase is not more than 3 % per log cycle of time. Samples S1 and S3 fall into this group, therefore no significant increase in v_s and G_{max} is expected. On the other hand, for sample S2, D_{50} < 0.04 mm, and thus, a significant increase could and indeed it occurs. Results of the BE tests on all three samples at different confinements are presented in Fig. 5. Fitted curves and their equations are also shown.

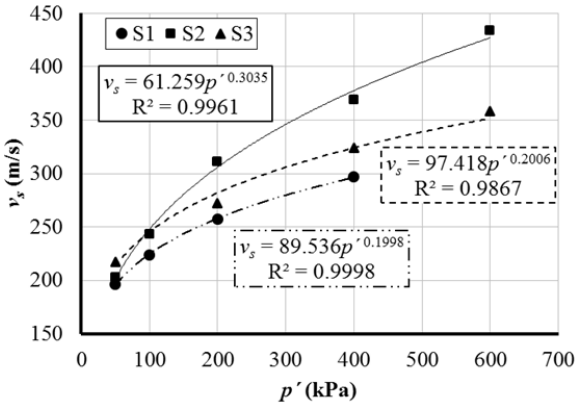


Fig. 5 Power relationship for v_s with respect to p' obtained from tested samples

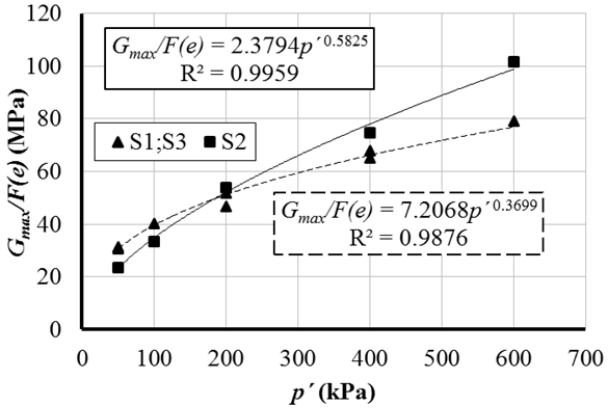


Fig. 6 Evolution of shear modulus normalized by void ratio with *p'*

It is clear from Fig. 5 that S1 and S3 show a similar trend in evolution of v_s vs. *p'*. More rapid increase in the value of v_s can be observed for confinements lower than 200 kPa which may be explained with the confinement being lower than the in-situ effective stresses [24]. Higher values of v_s for S3 are mainly caused by its lower void ratio.

It can be seen in Fig. 5 that despite the fact that all of the investigated soils from Layer V have similar physical parameters (index of plasticity, degree of saturation and specific density) there is a distinct difference in the evolution of v_s vs. *p'* for S2 and for the other two samples. This could be caused not just by the different void ratios as it will be demonstrated herein, but also by the different values of overconsolidation ratio, D_{50} (thus clay content) and in-situ state of stress. Based on geological literature, some slight level of overconsolidation may be expected in Layer V; however, measurement of OCR exceeded the scope of this study. Fabric and structure are not expected to play a significant role in this case [23].

Sample S3 showed highest v_s values in the range of higher confinements, while this tendency does not seem to extend to lower confinements. This could be caused by different degree of relaxation of the sample after removal from the in-situ stress conditions and small fissures or openings.

Different void ratios were observed across the soil profiles/boreholes on the site for the depths of the tested samples. Thus, it was necessary to obtain a range of values of v_s for different void ratios to incorporate this variation into the ground response calculations. This was done through normalization of G_{max} by a function of void ratio *F(e).* This function was chosen as (4) based on [23].

$$F(e)=(2.973-e)^2/(1+e) \quad (4)$$

Resultant plot with respect to mean effective stress *p'* is given in Fig. 6. Fitted curves and their constants *A* and *n* for obtaining G_{max} can be written in the form:

$$G_{max}=A\,F(e)\,p'^{n} \quad (5)$$

These equations were used for estimating the expected range of v_s for the different *p'* and void ratios to be used in the calculations. Further investigations will focus on the effects of duration of confinement, current stress state and OCR.

E. Resonant Column and Torsional Shear Testing

Samples from Layer II and Layer IV were investigated with RC and TOSS. A combined RC-TOSS device was used for testing which was built by Ray [25], [26]. It has been further developed since and used in previous studies at Győr [16], [27]. The benefit of the combined testing is that not only v_s or G_{max} can be determined as with the other test methods mentioned in this paper, but shear modulus degradation and damping curves can also be obtained.

The device has a fixed-free configuration which means the cylindrical sample is connected rigidly to a base platen and a loading system is placed on the top of the sample which consists of a top cap and a rod with four neodymium magnets. The magnets are individually surrounded by coils but they are free to move, therefore the sample is freely rotating around the vertical axis of the sample when a regulated flow of electricity in the coils cause the magnets to move. Hollow cylindrical samples are used for testing to insure a more even distribution of induced shear stresses and strains in the sample. Outer diameter of the samples is 6 cm, inner diameter is 4 cm, and sample height is 14 cm. It has to be noted, that due to sample thickness, soils with high gravel content cannot be tested with this device.

Samples of the coarse-grained soils of Layer II and Layer IV were obtained with a spiral auger; hence their in-situ state was clearly disturbed. In order to model their in-situ behavior reconstituted samples were used. State of compaction was estimated based on CPT results and loosest and most dense state was investigated in laboratory. Table IV summarizes physical properties of the tested samples.

TABLE IV
PHYSICAL PROPERTIES OF TESTED SAMPLES - RC-TOSS TESTS

Sample ID / depth (m)	State of compaction / saturation	Void ratio *e* (-)	Mean part. diam. d_m (mm)	Unif. coeff. C_U (-)	Conf. (kPa)
S4 / 5.0	med. dense / dry	0.64	0.2	2.0	65
S5 / 8.5	dense / saturated	0.76	0.18	2.1	115
S6 / 12.0	dense / saturated	0.54	0.35	1.9	140

Samples S4 and S6 were sands without almost any other fraction present, only ~5% gravel, while S5 had ~15% gravel. Due to sample size, the gravel fraction has been sieved out from S5. Since gravel content was relatively low even in S5, stiffness is expected to be governed by the soil skeleton built up by the sand grains. It has to be noted that, according to index tests and CPT results, Layer IV was fairly inhomogeneous throughout the site, and in many places, it was found to be more gravelly than the tested samples.

Samples S4 and S5 were prepared for testing with pouring it carefully into the mold with a funnel and then compacting it via vibration until reaching the in-situ state of compaction. Sample S6 was pluviated from 50 cm height to achieve a dense state. After this stage, 65 kPa vacuum confinement was applied and loading device as well as data acquisition system

Open Science Index, Geological and Environmental Engineering Vol:11, No:4, 2017 publications.waset.org/10006887/pdf

Open Science Index, Geological and Environmental Engineering Vol:11, No:4, 2017 publications.waset.org/10006887/pdf

was assembled and vacuum was kept on during testing as well. For higher confinement testing a pressure chamber was also used. All tests were performed with the samples being in an isotropic stress state.

For RC testing, a sine wave harmonic excitation is applied on the sample with a strain level of approx. 10^{-4} %. Response of the sample is captured with use of an accelerometer and oscilloscope. Using a manually governed frequency sweep, resonance can be found and with the physical properties of the sample and device known, shear wave velocity can be obtained [25]. After release of loading, the free decay can also be observed, and damping can be obtained with the logarithmic decrement method.

TOSS testing was performed in a stress controlled manner, during which proximitors are used for obtaining deformation of the sample. Data acquisition and test control were done with use of a self-developed VBA program [25]. Regular testing sequence consists of (i) RC measurements at lowest strain level for obtaining G_{max}, (ii) assessment of duration of confinement effects with repeated RC measurements (iii) TOSS testing with sine cyclic loading with sequentially increased amplitude to obtain modulus degradation curve, (iv) low strain RC test as control measurement to assess any changes in G_{max} due to TOSS testing. Duration of confinement was found to have no significant effect on v_s after a settling of approx. 30 minutes, during which a 2-3% increase could be observed.

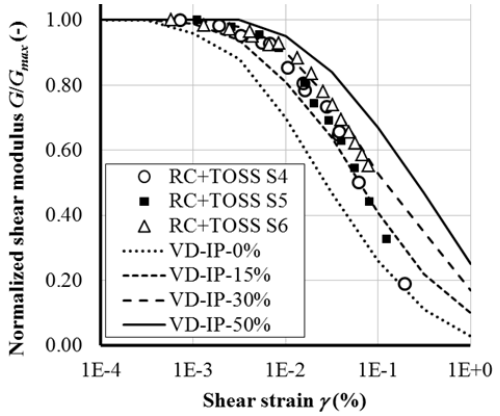


Fig. 7 Modulus degradation curves obtained with RC+TOSS tests

Fig. 7 shows obtained degradation curves compared to often cited curves presented by [26]. Although fines content of tested samples was negligible (1% for S4 and S5, 3% for S6), obtained results seem to fit with curves given for soils with an index of plasticity between 15% and 30%.

III. Comparison of Site Investigations and Laboratory Tests

After performing the different tests described in Chapter II, careful evaluation was conducted and results were compared.

Fig. 3 shows a fairly good agreement overall between profiles obtained with MASW and SCPT. In the SCPT profiles, a rapid increase in v_s around 12 and 21 m suggests thin layers of gravel which is difficult to detect with MASW. However, the deposition of coarse grained fractions on the top surface of the Miocene clays around 12 m is plausible according to geological descriptions.

Fig. 4 shows a very good agreement overall between SCPT measurements and estimated v_s values based on correlations using regular CPT data. A bigger scatter in both the estimated and measured v_s can be found in Layer IV which is due to the non-homogeneity of the gravelly sand layers in terms of grain size distribution and especially gravel content.

Shear wave velocity values obtained with BE, RC, and TOSS measurements provided a lower bound of the in-situ tests. In terms of BE tests, this may be due to disturbances connected to sampling, transfer of samples, and relaxation. Effects of confinement duration may also be a reason behind lower values of v_s as also reported in [24]. For RC and TOSS tests, the uncertainties about in-situ void ratio (state of compaction) and stress state may be a reason behind the differences.

When comparing laboratory and field measurements, one has to carefully assess in-situ stress state in order to connect confinement levels in laboratory tests to depth below ground surface in reality. At this site, the groundwater table was found 6 m below surface and as expected, granular soils of Layers I-IV were saturated according to tests performed on the samples taken from the boreholes. Based on this, effective stresses should be calculated when comparing lab and in-situ results. However, it is much more difficult to assess the stress state in the clays of Layer V, especially if one wishes to assess stress levels of deeper layers (50-100 m) which was necessary at this site for the ground response analysis. Since the permeability of these soils is many orders of magnitude smaller than those above, one could argue that they can be considered impermeable and a total stress approach has to be taken. However, if the ground water table can be considered permanent, which is the case here, one could assume a saturated state even for deeper layers if one thinks about geological time scales for achieving saturation and an effective stress approach should be used.

Fig. 8 shows a summary of all tests with averaged v_s values for the main layers. BE tests performed at a confinement corresponding to sample depth are shown with black triangles. Lower and higher confinement results were used for estimating v_s for regions above and below the sample depth.

Based on the investigations performed with different methods, five 1D models have been developed for ground response analysis. Model A is based on SCPT results. Model B is based on MASW results. Models C and D were obtained with use of regular CPT data and correlations detailed in Chapter II/C. For Model D, a CPT profile was used which showed a significant presence of the organic Layer III while Model C used the CPT data of one of the SCPT tests. Model E was based on the laboratory tests (BE, RC, and TOSS). Fig. 9 shows the five models.

Open Science Index, Geological and Environmental Engineering Vol:11, No:4, 2017 publications.waset.org/10006887/pdf

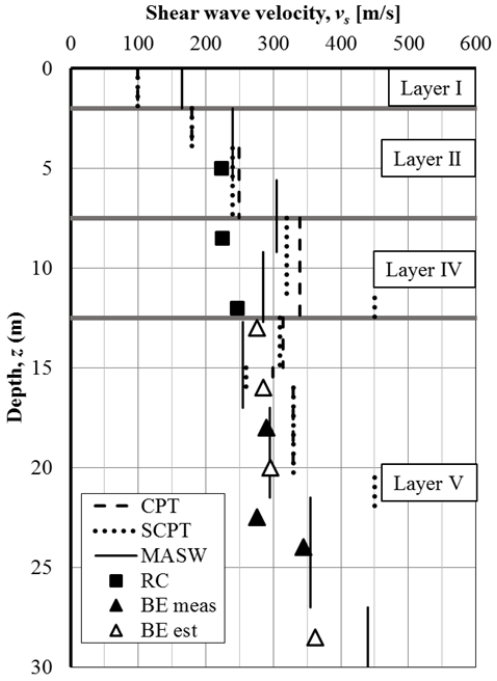


Fig. 8 Comparison of obtained shear wave velocity values

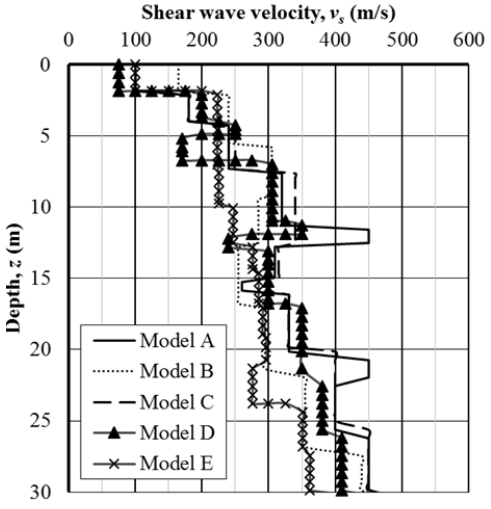


Fig. 9 Soil stratification models obtained with different test methods

IV. Ground Response Analysis

Seismologists and earthquake engineers usually divide the problem of seismic wave transmission from the earthquake source to the investigated structure into four stages: (i) source, (ii) geologic path through rock layers, (iii) near surface path through soil and surficial rock layers, and (iv) interaction between shallow soil and structure. This paper focuses on the third stage. More details of the method can be found in [28].

Simplifications to site response analysis often reduce the problem to one dimension and a single type of wave: horizontally-polarized vertically-propagating shear wave. This corresponds to the most damaging wave for buildings. The horizontal motion imparts lateral inertia loads on the building, which are generally more difficult to resist than vertical loads. The vertical propagation is a reasonable approximation as well since the pathway for seismic waves becomes more vertical as it moves through material that is less stiff (lower v_s, G_{max}) as it moves toward the surface.

A. Rexel Software

For choosing earthquake records to be used in the ground response analysis calculations, the software package Rexel [29] was used. The software uses a magnitude scaling technique which means strong motion records are selected from a database (European Strong-Motion Database) and compared to a desired set of criteria. If the record meets the criteria, it is copied into a "bin" of motions that will be used later. For many typical low to moderate seismic actions, the database will contain many suitable records. However, if the criteria are not met, Rexel will scale the earthquake motion (increase or decrease acceleration amplitude) so that it will meet the criteria. While amplitude scaling has some disadvantages, especially with frequency content, records that are nearly the same magnitude will be accurate enough. Other parameters affect the suitability of an earthquake for scaling and relocation. Distance from epicenter and type of faulting that initiated the motion all have an impact on the final behavior in the response analysis.

The most common set of criteria are those described by Eurocode 8 or other building code standards. Design spectra from these codes are easily input to the program, and default values of allowed variability are often enough to produce a bin of seven earthquake records that are subsequently used in the soil response analysis program as input motions on the bedrock. Therefore, it is common to use records which were obtained at locations where the layers close to the surface are rock-like, i.e. quite stiff, because these layers will modify (filter or amplify) the base rock motion the least. Such sites are usually classified into class A by Eurocode 8. For this study, three bins of seven earthquake records were selected; two that match EC 8 Type 1 spectrum (denoted later as T1a and T1b) and one for the Type 2 spectrum (denoted as T2), all of them for a site class A.

B. Strata Software

For the ground response analysis, the software Strata [30] was used. This program uses a 1D equivalent-linear approach, meaning nonlinear response of the soil is approximated by modifying the linear elastic properties of the soil based on the induced strain level, and then iteratively calculated based on the computed strain. A transfer function is used to compute the shear strain in the layer based on the input motion. The computational method of Strata is very efficient; a large number of soil profiles, earthquakes and soil nonlinear conditions can be examined. Soil profiles can be varied by specifying mean and standard deviation values of shear stiffness G_{max} and damping D for each soil layer.

All earthquake motions (21 this case) can be specified initially and the software will collect all results and compute profile data, response spectra, transfer functions, and time histories with median, high and low percentile or log standard

Open Science Index, Geological and Environmental Engineering Vol:11, No:4, 2017 publications.waset.org/10006887/pdf

deviations. Therefore, the impact of the variability of input data on site response can be quantified. For this study, we performed calculations (i) with the use of the obtained five models without any variation allowed; (ii) with the variation of v_s in each layer based on the scatter of the measurements (10 profiles); (iii) with the variation of layer thickness (10 profiles); (iv) with the variation of both v_s and layer thickness (50 profiles); (v) with the variation of v_s, layer thickness and nonlinear parameters (100 profiles). Since in geotechnical engineering practice v_{s30} has to be assessed for seismic design, in many cases, only the top 30 m of soil layers is investigated. Therefore, we performed all calculations with the obtained five models and assuming 30 m as the depth of the bedrock; and we also compared these to calculations with deeper models where we used a power function to estimate deeper layer's v_s based on the measurements done in Layer V. For these runs, depth of bedrock was taken as 110 m based on deep boreholes from the surrounding area and geological descriptions. For all five models, the same evolution of v_s was assumed between 30 m and 110 m.

As mentioned in Chapter I, based on the Seismic Hazard Map of Hungary the expected level of PGA is 0.14 g at bedrock with 10% probability of exceedance in case of the Significant Damage (SD) limit state. According to Eurocode, three limit states should be taken into account for the evaluation of earthquake resistance of buildings, which form the basis for scenario preparation. Therefore, we performed all (v) calculations with a PGA of 0.11 g and 0.24 g beside the regular 0.14 g as well in order to check limit states of Damage Limitation (DL) and Near Collapse (NC), respectively. Altogether, nearly 78 000 realizations were calculated.

C. Results

In the following section, the main results of some calculations are presented for selected models. Tendencies were similar for all models; however, clarity and space constraints would not allow presentation of more results. All calculated spectra are mean values of the calculated variations.

Fig. 10 shows the effect of different input motions. T1a and T1b contained 7-7 earthquake records fitting the EC8 Type I C spectrum; T2 contained seven earthquakes fitting the EC8 Type II C spectrum. It can be observed that all spectra show much higher peaks than the EC8 spectra, and also shapes of the spectra are much wider than EC8 spectra. Average values of ~0.6 g spectral accelerations can be observed in the range of engineering structures (0.3-1.0s period).

Fig. 11 shows how parameter variation affects the acceleration response spectrum at this site. Starting from one profile (nothing varied) with the highest peak as variation is introduced, peaks of spectral acceleration reduces gradually. When considering a deep profile (110 m) which can be considered more realistic, although a fair amount of estimation has to be made in terms of input parameters, a much lower and wider spectrum is obtained.

One of the main results of this study is shown in Fig. 12 which compares three 30 m deep models based on the different investigation methods. A very good agreement could be found between the spectra obtained with Model B and E (MASW and laboratory tests), while Model A (SCPT) gave a similar spectrum with a much higher peak.

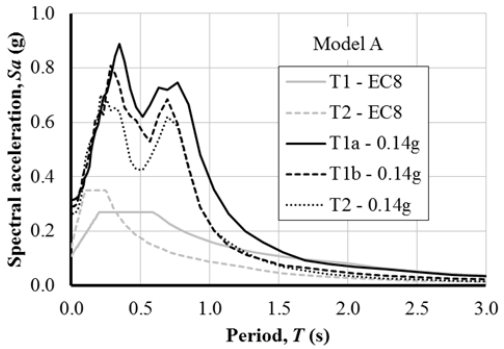


Fig. 10 Acceleration response spectra for different EQ motions

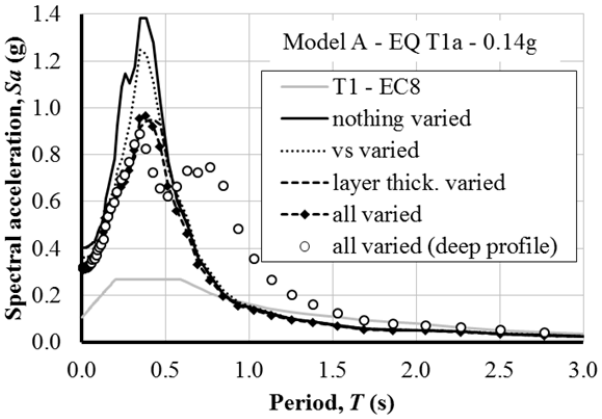


Fig. 11 Acceleration response spectra with parameter variations

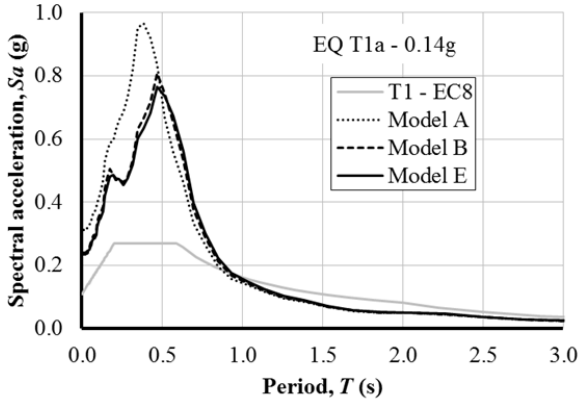


Fig. 12 Acceleration response spectra comparing SCPT (Model A), MASW (Model B) and laboratory measurement (Model E) based soil profiles with 30-m models

A better agreement can be found between the spectra in Fig. 13 that shows the results for the same three models as Fig. 12 but with a more realistic, deeper model (110 m). Again, very high spectral accelerations and a wide spectrum can be observed.

Fig. 14 shows the effect of input PGA level. Interestingly PGAs of 0.11 g and 0.14 g show spectral accelerations of

similar magnitude, while the 0.24 g curve is showing enormously high accelerations.

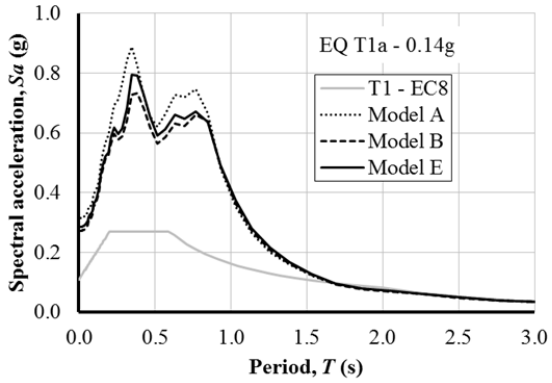


Fig. 13 Acceleration response spectra comparing SCPT (Model A), MASW (Model B) and laboratory measurement (Model E) based soil profiles with 110-m models

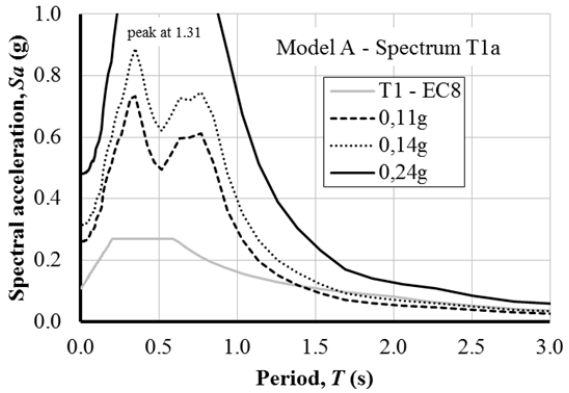


Fig. 14 Acceleration response spectra comparing different PGA levels

The CPT based estimated Model C shows very good agreement with the SCPT based Model A as shown in Fig. 15. Again, the effect of model depth can be observed: shallow models tend to give a single higher peak in the spectral accelerations, while the deeper models result in wider spectra.

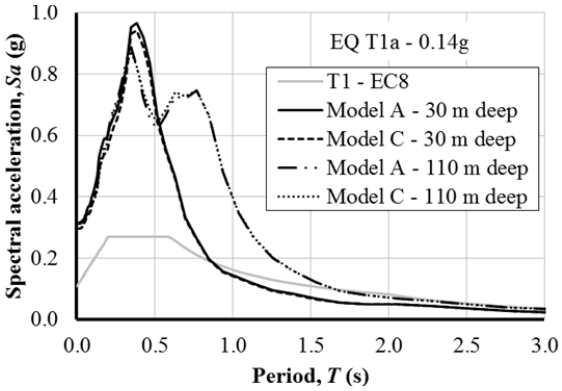


Fig. 15 Acceleration response spectra comparing SCPT (Model A), regular CPT (Model C) based soil profiles

The presence of the organic layer has a significant effect on ground response according to Fig. 16. Model D was based on a CPT profile which showed the presence of the organic layer clearly; its spectrum has a lower plateau than that of Model C.

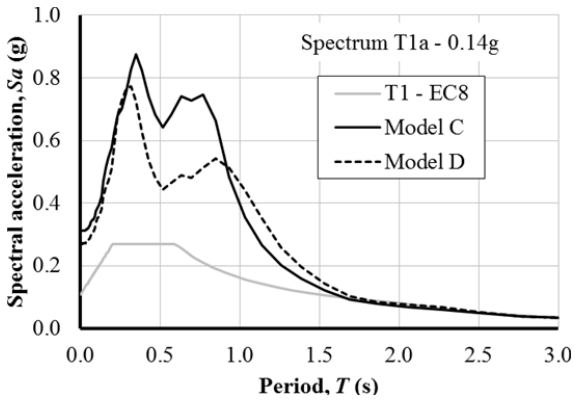


Fig. 16 Acceleration response spectra showing the effect of the presence of organic Layer III (Model D is with organic layer)

Based on the calculations, we can conclude that characteristics of the obtained spectra are different from that of the Eurocode 8 spectra both in shape and level of spectral acceleration. Levels of 0.6-0.8 g spectral accelerations were found to be common in the results which strongly suggest that further studies have to be made in this field.

V. Conclusions

In this paper, the effect of site investigation methods on ground response analysis results has been showed through a case study in Budapest, Hungary. Different test methods have been used, and based on them, five separate soil models have been developed for the investigated site. 1D equivalent linear ground response analyses have been performed, and results have been compared to EC8 spectra.

All testing methods proved their applicability and provided a complex view on the given site. All tests have their pros and cons, and these must be considered before detailed geological surveys are conducted.

Although a site with PGA level of 0.14 g was investigated, very high spectral accelerations have been found, which suggests that surface near soil layers have a major effect on earthquake loading.

Further studies will be focusing on extended Bender Element testing to assess duration of confinement effects; comparison with Bender Element and Resonant Column Testing; and ground response analysis calculations with different software packages.

References

[1] CEN European Committee for Standardization: MSZ EN 1998-1:2008 Design of structures for earthquake resistance, Part 1 General rules, seismic actions and rules for buildings, pp. 1-216.

[2] Kegyes-Brassai, O. 2015. *Earthquake Hazard Analysis and Building Vulnerability Assessment to Determine the Seismic Risk of Existing Buildings in an Urban Area*, PhD Dissertation. Széchenyi István University, 199 p.

Open Science Index, Geological and Environmental Engineering Vol:11, No:4, 2017 publications.waset.org/10006887/pdf

[3] Dorman, J. & Ewing, M., 1962. *Numerical inversion of seismic surface wave area, dispersion data and crust-mantle structure in the NewYork-Pennsylvania,* J. geophys. Res. *1962,* 67, pp. 5227–5241.
[4] Aki, K. and Richards, P.G., *Quantitative Seismology.* W. H. Freeman & Co., San Francisco. 1980.
[5] Park, C.H., Miller, R.D. and Xia, J., *Multichannel analysis of surface waves,* 1999, Geophysics, 64, pp. 800–808.
[6] O. Yilmaz., *Seismic data processing.* Society of Exploration Geophysics, Tulsa, 1987, pp. 62-79.
[7] C.B. Park, J. Xia and R.D. Miller. "Imaging dispersion curves of surface waves on multichannel record" in *68th Annual International Meeting of Society of Exploration Geophysics*, Expanded Abstracts, 1998, pp. 1377-1380.
[8] Kanlı, A. I., Tildy, P., Prónay, Z., Pınar, A., and Hermann, L., *Vs30 mapping and soil classification for seismic site effect evaluation in Dinar region, SW Turkey*: 2006, Geophys. J. Int., 165, pp. 223-235.
[9] Radex Pro Software, Deco Geophysical Inc., www.radexpro.com last access March 10, 2017.
[10] P. Robertson. 2009. Interpretation of cone penetration tests - a unified approach. Canadian Geotechnical Journ., Vol 46., pp. 1337-1355.
[11] R.D. Andrus, N.P. Mohanan, P. Piratheepan B.S. Ellis and T. L. Holzer, "Predicting shear wave velocity from cone penetration resitance", in *Proceedings, 4th International Conference on Earthquake Geotechnical Engineering, Thessaloniki, Greece, Paper No. 1545, 2007.*
[12] Á. Wolf and R.P. Ray, Comparison and Improvement of the Existing Cone Penetration Test Results – Shear Wave Velocity Correlations for Hungarian Soils, *Proceedings of ICEES 2017: 19th International Conference on Earthquake Engineering and Seismology,* Paris, 2017, submitted for publication.
[13] P.K. Robertson and C.E. Wride, "Evaulating cyclic liquefaction potential using the cone penetration test, Canadian Geotechnical Journal, Vol. 35. pp 442-459.
[14] P. D. Greening, D.F.T. Nash, „Frequency domain determination of G_0 using bender elements", in *Geotechnical Testing Journal*, Vol. 27, No. 3, West Conshohocken, PA: ASTM International, 2004, pp. 288-294.
[15] R. Dyvik, C. Madshus, „Lab measurements of G_{max} using bender elements." *Proceedings of the Conference on the Advances in the Art of Testing Soil under Cyclic Conditions*, ASCE Geotechnical Engineering Division, New York, 1985, pp. 186-196.
[16] Z. Szilvágyi, P. Hudacsek, R.P. Ray, 2016. Soil shear modulus from Resonant Column, Torsional Shear and Bender Element Tests. *In International Journal of Geomate 10:(2),* pp. 1822-1827.
[17] M.L. Lings, P.D. Greening, „A novel bender/extender element for soil testing.", in *Géotechnique*, Vol. 51, No. 8, London: Thomas Telford Ltd., 2001, pp. 713-717.
[18] T. Ogino, T. Kawaguchi, S. Yamashita, S. Kawajiri. „Measurement deviations for shear wave velocity of bender element test using time domain, cross-correlation, and frequency domain approaches.", in *Soils and foundations*, Vol. 55, No. 2, Amsterdam: Elsevier B.V., 2015, pp. 329-342.
[19] A. Viana da Fonseca, C. Ferreira, M. Fahey, „A framework interpreting bender element tests, combining time-domain and frequency-domain methods", in *Geotechnical Testing Journal,* Vol. 32, No. 2*,* West Conshohocken, PA: ASTM International, 2009 pp. 1-17.
[20] V. Jovicic, M.R. Coop, M. Simic, „Objective criteria for determining G_{max} from bender elements", in *Géotechnique*, Vol. 46, No. 2, London: Thomas Telford Ltd., 1996, pp. 357-362.
[21] G. Viggiani, J.H. Atkinson, „Stiffness of fine grained soils at very small strains.", in *Géotechnique*, Vol. 45, No. 2, London: Thomas Telford Ltd., 1995, pp. 249-265.
[22] S. S. Afifi, F.E. Richart, „Stress-history effects on shear modulus of soils" in *Soils and foundations*, Vol. 13, No. 1, Amsterdam: Elsevier B.V., 1973, pp. 77-95.
[23] B.O. Hardin, W. Black, Vibration modulus of normally consolidated clay.", in *Journal of Soil Mechanics and Foundations Divison*, Vol. 94, No. 2, Reston, VA, ASCE, 1968, pp. 353-369.
[24] K. Stokoe, F. Richart, „Shear moduli of soils, in-situ and from laboratory tests." *In WCEE, editor, 5th World conference in earthquake engineering*, Rome, Italy, 1973, pp. 356–359.
[25] R.P. Ray. 1983. *Changes in Shear Modulus and Damping in Cohesionless Soil due to Repeated Loadings*, Ph.D. dissertation, University of Michigan, Ann Arbor, MI., 417 pp.
[26] R. P. Ray, R.D. Woods. 1987. Modulus and Damping Due to Uniform and Variable Cyclic Loading in *Journal of Geotechnical Engineering, Vol. 114, No. 8.* ASCE, pp. 861-876.
[27] R. P. Ray, Z. Szilvágyi, 2013. Measuring and modeling the dynamic behavior of Danube Sands. In *Proceedings 18th International Conference on Soil Mechanics and Geotechnical Engineering: Challenging and Innovations in Geotechnics.* Paris, Presses des Ponts pp. 1575-1578.
[28] O. K. Kegyes-Brassai & R. P. Ray, 2015 Comparison of the 1D response analysis results of typical Hungarian soil types and the EC8 spectra based on a case study of seismic risk analysis in Győr. WIT Transactions on The Built Environment, Vol 152, pp111-122.
[29] I. Iervolino, C. Galasso, E. Cosenza, 2009 REXEL: computer aided record selection for code-based seismic structural analysis, Bull Earthquake Eng (2010) 8:339–362.
[30] A. Kottke, X. Wang, E. M. Rathje. 2013 NEEShub Resourses: Strata (Online, accessed at 03.19.2017) available at https://nees.org/resources/strata.

Open Science Index, Geological and Environmental Engineering Vol:11, No:4, 2017 publications.waset.org/10006887/pdf